AJNR

Three-Dimensional Rotational Spinal Angiography in the Evaluation and Treatment of Vascular Malformations

Charles J. Prestigiacomo, Yasunari Niimi, Avi Setton and Alejandro Berenstein

AJNR Am J Neuroradiol 2003, 24 (7) 1429-1435
http://www.ajnr.org/content/24/7/1429

AJNR Am J Neuroradiol 24:1429–1435, August 2003

Three-Dimensional Rotational Spinal Angiography in the Evaluation and Treatment of Vascular Malformations

Charles J. Prestigiacomo, Yasunari Niimi, Avi Setton, and Alejandro Berenstein

BACKGROUND AND PURPOSE: **Conventional spinal angiography, although useful in providing angioarchitectural details of spinal vascular disease, has limitations. The advent of 3D angiography has provided a better comprehension of angioarchitectural detail when evaluating the intracranial circulation. The purpose of this study was to evaluate the usefulness of 3D angiography in the diagnosis and treatment of vascular malformations of the spine.**

METHODS: **This retrospective analysis included 17 3D spinal angiograms acquired in 14 consecutive patients examined at our institution for a spinal vascular lesion, which included nine spinal cord arteriovenous malformations (AVMs), one perimedullary arteriovenous fistula (AVF), three spinal dural AVFs, and one nerve root AVM. 3D angiography was obtained with apnea under general anesthesia by using a 14-second acquisition and 200° rotation of the gantry during injection of 300 mg I/mL nonionic contrast material at a rate of 0.5–3.5 mL/s. Multiple reconstructed images were obtained with or without opacification of the surrounding structures. These images were then evaluated by the interventionalists at the time of the procedure and compared with findings obtained by conventional subtraction angiography.**

RESULTS: **3D angiography was useful in differentiating intramedullary lesions from perimedullary surface lesions; detecting arterial, nidal, or venous aneurysms; and evaluating the 3D structure of the lesion as well as the relationship between the malformation and its draining veins or surrounding bony structures. In specific situations, it obviated the need for contrast-enhanced conventional or 3D CT, as well as for lateral or oblique angiographic views, which are sometimes difficult to obtain with good quality. No 3D angiography–related complications were experienced. Some limitations in the definition of small vessel anatomy in the reconstructed images were noted.**

CONCLUSION: **In this small series of patients, 3D angiography was safe and useful for evaluation of the 3D vascular anatomy of spinal vascular malformations.**

The diagnosis and management of vascular malformations of the spine and spinal cord have undergone significant development since they were first recognized as a clinical entity in 1888 (1). The precise preoperative delineation of the angioarchitecture of spinal cord vascular lesions, however, did not take place until the development of selective spinal angiography, as engineered by Djindjian, Di Chiro, Doppman, and others (2–4). Additional advances in nonionic contrast media, real-time digital subtraction fluoroscopy, and catheter technology have made spinal angiography safer and more sensitive in detecting vascular disease. Recently, 3D rotational acquisition and reconstruction angiography has given investigators the ability to better understand the 3D relationships that exist when studying aneurysms and other vascular anomalies (5, 6). 3D rotational angiography of the spinal cord (3D rotational spinal angiography, or 3D-RSA) provides a high-resolution 3D representation of spinal angioanatomy and the vessels' location relative to spinal cord and surrounding structures. We present a series of 14 consecutive patients with spinal vascular malformations who presented for spinal angiography, 3D-RSA, and treatment at our institution.

Received October 7, 2002; accepted after revision February 18, 2003.

From the Center for Endovascular Surgery, Beth Israel Medical Center, Singer Division, New York, NY (Y.N., A.S., A.B.), and the Departments of Neurological Surgery and Radiology, University of Medicine and Dentistry of New Jersey, Newark, NJ (C.J.P.).

Address correspondence to Yasunari Niimi, M.D., Center for Endovascular Surgery, Herbert and Nell Singer Division, Beth Israel Medical Center, 170 East End Avenue at 87th Street, New York, NY 10128.

Methods

Conventional Digital Subtraction Spinal Angiography

Between November 2000 and January 2002, 14 patients presented to our institution for selective diag-

Patient characteristics

Patient (no.)	Age (y)/Sex	Diagnosis	Location	Feeders	Catheter Location	3D-RSA Benefits*
1	20/M	Spinal cord AVM	Cervical	C3–C5 (ASA); right DA (radiculomedullary); left C6 (PSA); right VA (LSA)	Left VA	1, 2
2	10/M	Spinal cord AVM	Cervical	Bilateral VA (ASA and PSA)	Right VA	2
3	14/M	Spinal cord AVM	Cervical	Right DA (ASA)	Right DA	1, 2
4	26/F	Spinal cord AVM	Conus	Left T10 (ASA); right L2 (PSA); left T11 (PSA)	Left T10 IA	2, 3
5	26/F	Spinal cord AVM	Cervical	Left VA (ASA); right DA (ASA and PSA)	Left VA	1, 2
6	18/M	Spinal cord AVM	Cervical	C1–C2 (ASA); right C2 (LSA)	Left VA	1, 2, 3
7	34/M	Perimedullary spinal AVM	Cervical	Left C6 (ASA)	Left VA	1, 2, 3
8	54/M	Spinal dural AVF	Thoracic	Left T12	Left T12 IA	3, 4
9	45/F	Spinal cord AVM	Cervical	Right C4 (ASA); left C5 (ASA)	Right VA; left T4 IA	2
10	69/F	Spinal dural AVF	Thoracic	Right T7	Right T7 IA	2, 3, 4
11	49/M	Spinal cord AVM	Cervical	Right SA (ASA)	Right SA	1, 2
12	63/M	Nerve root AVM	Cervical	Left C5; right C5 (PSA)	Left C5 RA	2, 3, 4
13	51/F	Spinal cord AVM	Cervical	Right C3 (ASA); left PICA (LSA)	Right VA	1, 2
14	46/M	Spinal dural AVF	Lumbar	Left L1	Left L1 artery	2, 3, 4

Note.—AVM signifies arteriovenous malformation; ASA, anterior spinal artery; PSA, posterior spinal artery; VA, vertebral artery; LSA, lateral spinal artery; DA, dorsovervical artery; IA, intercostals artery; AVF, arteriovenous fistula; SA, subclavian artery; RA, radicular artery; and PICA, posterior inferior cerebellar artery.

* 1, visualization of aneurysm; 2, definition of angioarchitecture; 3, visualization of relationship to surrounding structures; and 4, need for CT to confirm location of embolic agent obviated.

nostic spinal angiography and treatment of vascular lesions of the spine and spinal cord. The Siemens Neurostar Plus system (Siemens, Erlangen, Germany) was used for all procedures. All patients underwent selective spinal angiography under general anesthesia with electrophysiologic monitoring consisting of somatosensory evoked and motor evoked potentials. All conventional digital subtraction angiography (DSA) was performed with a 1024 × 1024-pixel matrix system with road-mapping function. Biplane studies were performed only when good beam penetration could be achieved on lateral projections (eg, cervical lesions).

3D Rotational Spinal Angiography

Data were acquired in a 1024 × 1024 matrix with a field of view of 33 inches and a large focal spot. A 14-second acquisition protocol under apnea was performed through a 200° rotation of the C-arm. A 1–2 mL/s injection of the artery of interest was performed with injection of 300 mgI/mL nonionic contrast medium at a pressure of 300 psi. This technique was modified when superselective rotational angiography was performed for which a 0.5 mL/s injection was used at a pressure of 450 psi. In the brachiocephalic vessels, 3.0–3.5 mL/s contrast medium was injected at a pressure of 300 psi. This 132-image study was then transferred to a Siemens Virtuoso workstation in native or subtracted format and processed by experienced neuroradiology technicians with the assistance of the operating interventionalists (C.J.P., Y.N., A.S., A.B.). If the patient had previously undergone embolization and had radiopaque N-butyl cyanoacrylate (NBCA) casts, images were transferred in subtracted format to evaluate remaining flow accurately. Reconstructed images, including maximum intensity projection images, shaded surface-rendered displays, and volume-rendered displays with adjustable transparency of various structures, as well as full stereoscopic capabilities, were used to study the anatomic relationships demonstrated on these images.

The reconstructed images were then evaluated by the operating interventionalists (CJP, YN, AS, AB) and compared with the conventional subtraction angiograms, with particular attention paid to the 3D anatomic relationships of the vasculature and the surrounding structures.

Results

Fourteen patients underwent conventional spinal angiography for the evaluation and treatment of various vascular malformations of the spine and spinal cord. The Table briefly describes the distribution and description of the lesions. 3D-RSA was performed at the level of the noted lesion to better delineate the angiographic anatomy and relationship to surrounding structures. Electrophysiologic monitoring before and after rotational angiography was unchanged, and no complications secondary to the 3D-RSA were noted.

3D-RSA findings correlated with those of conventional DSA images to a measured vessel resolution of approximately 1 mm. Postprocessing of the reconstructed images allowed for partial opacification of the vertebral bodies and spinal cord, which provided the necessary anatomic landmarks for the vascular lesion and its surrounding relationships. In particular, when oblique and lateral views were difficult to obtain, 3D-RSA was able to help the interventionalists

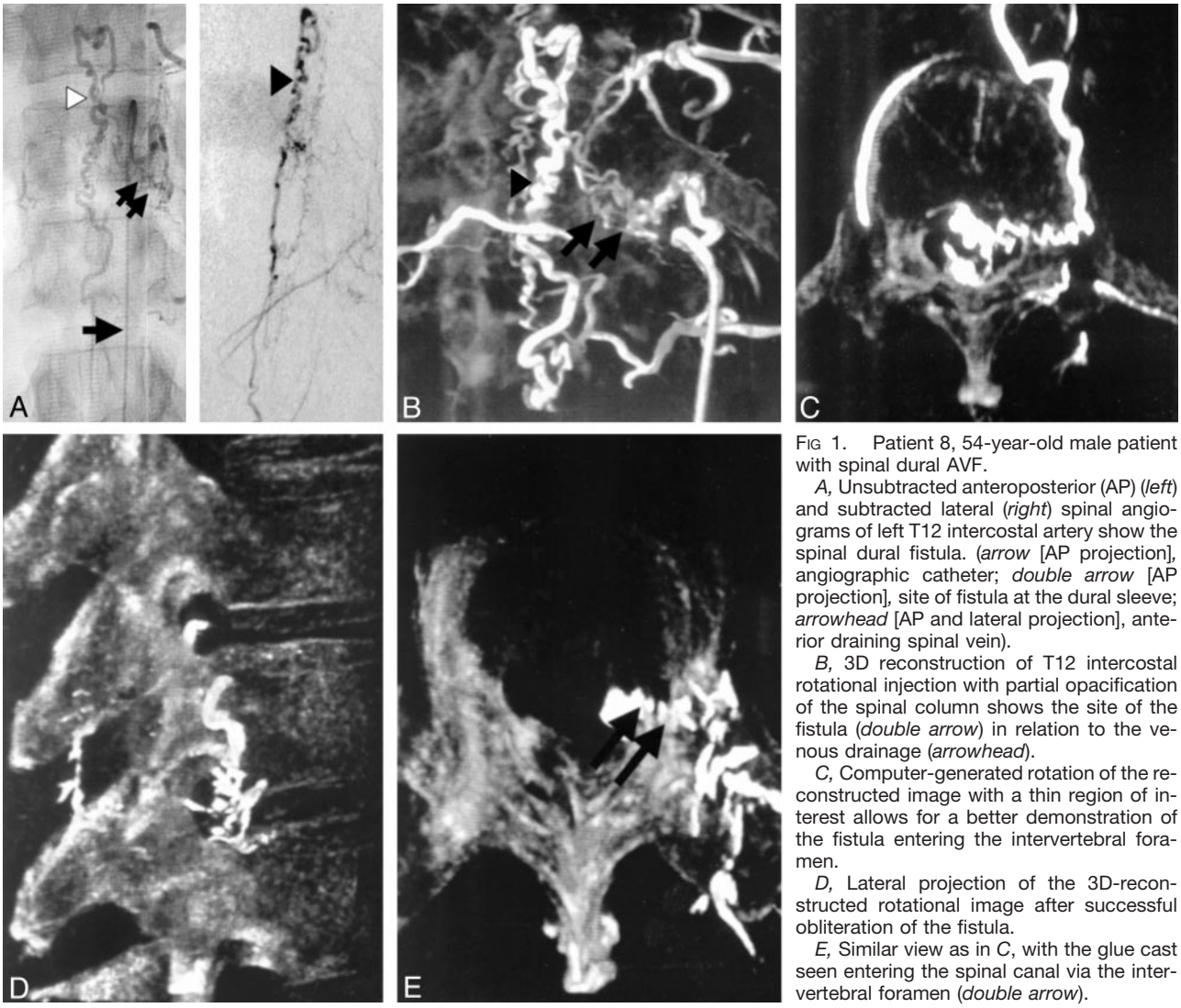

FIG 1. Patient 8, 54-year-old male patient with spinal dural AVF.

A, Unsubtracted anteroposterior (AP) (*left*) and subtracted lateral (*right*) spinal angiograms of left T12 intercostal artery show the spinal dural fistula. (*arrow* [AP projection], angiographic catheter; *double arrow* [AP projection], site of fistula at the dural sleeve; *arrowhead* [AP and lateral projection], anterior draining spinal vein).

B, 3D reconstruction of T12 intercostal rotational injection with partial opacification of the spinal column shows the site of the fistula (*double arrow*) in relation to the venous drainage (*arrowhead*).

C, Computer-generated rotation of the reconstructed image with a thin region of interest allows for a better demonstration of the fistula entering the intervertebral foramen.

D, Lateral projection of the 3D-reconstructed rotational image after successful obliteration of the fistula.

E, Similar view as in *C*, with the glue cast seen entering the spinal canal via the intervertebral foramen (*double arrow*).

determine the anteroposterior relationships between the various vascular structures.

Case Reports

Case 1 (Patient 8 [Table])

A 54-year-old right-handed obese male patient (weighing >300 pounds) with a 5-year history of low back pain presented with rectal pain, right leg hypesthesia, and right leg paresis on exertion of 1-year duration. Several months before treatment, he noted occasional priapism and urinary hesitation. MR imaging with T2-weighted imaging demonstrated hyperintensity within the conus and serpentine flow voids on the anterior and posterior surface of the lower spinal cord. The patient underwent conventional spinal angiography, which confirmed the presence of a spinal dural arteriovenous fistula with primary supply from the left T12 intercostal artery (Fig 1A). Two feeding pedicles were identified with a single radicular vein draining to a perimedullary vein at the T11 level. Drainage proceeded superiorly and inferiorly along perimedullary veins. 3D-RSA with injection of the left T12 intercostal artery clearly demonstrated the fistula's drainage inferiorly via anterior perimedullary veins and superiorly via posterior perimedullary veins (Fig 1B). By selecting a thin region of interest in the reconstructed image with partial opacification of bone, the intervertebral foramen through which the fistula entered the spinal canal was identified (Fig 1C). Successful obliteration of the fistula was achieved by deposition of NBCA into the fistula with penetration to the radicular vein. Rotational imaging of the glue cast was performed, which confirmed the location of the glue cast in relation to the osseous anatomy (Fig 1D and E).

3D-RSA was beneficial in this patient for several reasons. By adjusting the relative opacity of the bone, the site of fistula was localized to the root sleeve at the level of the foramen. In addition, because of the patient's obesity, oblique views to help distinguish anterior from posterior draining vessels was difficult. The ability to acquire a 3D imaging study precluded the need for multiple oblique projections. Finally, a

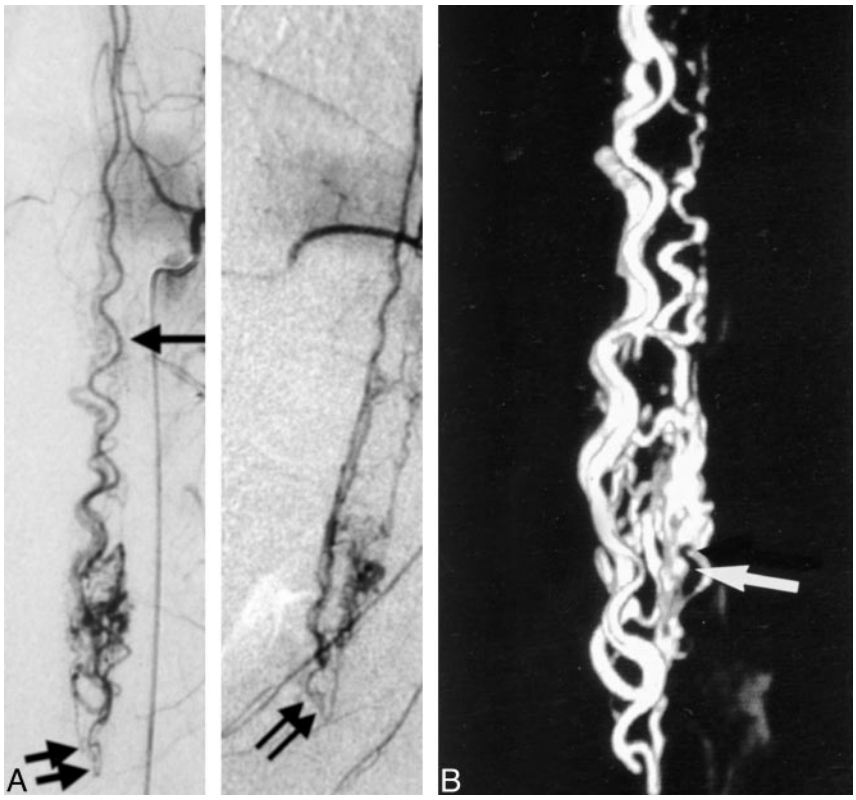

FIG 2. Patient 4, 26-year-old female patient with spinal cord AVM.

A, AP (*left*) and lateral (*right*) subtracted spinal angiograms from the left T10 intercostal artery, demonstrating the supply to this conus AVM from the anterior spinal artery (*arrow* [AP projection]). Lazorthe's basket is identified at the tip of the conus (*double arrows* [AP and lateral projections]).

B, 3D-RSA in the lateral projection shows several feeders to this primarily superficial pial malformation (*arrow*).

postembolization rotational image with partial opacification of the surrounding bone obviated the need for postoperative CT to localize the glue cast.

Case 2 (Patient 4 [Table])

A 26-year-old right-handed female patient presented with dysesthesias of the soles of her feet for approximately 1 year. MR imaging demonstrated prominent signal intensity voids on the anterior and posterior surface of the entire spinal cord with enhancement and hyperintense T2 signal abnormality in the region of the conus. Angiography demonstrated a small spinal cord AVM on the posterior surface of the conus supplied primarily from the anterior spinal artery (Fig 2A). Indirect supply from bilateral posterior spinal arteries at L1 was noted. 3D-RSA confirmed the superficial nature of the nidus and demonstrated the anterior and posterior drainage pattern for this lesion (Fig 2B).

The rotational study performed in this individual confirmed that this lesion was indeed superficial, as evidenced by partial opacification of the spinal cord at the level of the lesion. The anterior spinal vein was also clearly identified on these rotational images. The anterior spinal artery–posterior spinal artery anastomoses (Lazorthe's basket) was also identifiable on these images.

Case 3 (Patient 1 [Table])

A 20-year-old male patient initially presented 10 years ago with acute hematomyelia secondary to a cervical spinal cord AVM. He underwent embolization at that time with partial occlusion of the malformation. He presented with a second episode of hematomyelia and therefore underwent spinal angiography. At angiography, the residual malformation was noted with primary supply from the cervical branches of the vertebral artery (Fig 3A). Several oblique projections failed to delineate the true tortuous course of these feeders. For instance, the second principle feeder to the malformation in Figure 3A cannot be adequately separated from the vertebral artery. 3D-RSA was then performed, which clearly demonstrated the tortuous nature of these feeding pedicles (Fig 3B). Therefore, superselective angiography was performed, and after successful provocative testing, NBCA was deposited within the feeding pedicle.

The benefit of the 3D-RSA in this case enabled the interventionalists to select a feeder most feasible for embolization as well as to better understand how to safely navigate the feeding vessel by recognizing the significant tortuosity.

Case 4 (Patient 13 [Table])

A 51-year-old female patient initially presented with interscapular pain. MR imaging demonstrated an intramedullary spinal cord AVM of the upper cervical spine. Conventional angiography confirmed the supply of this malformation to be from the anterior spinal artery (Fig 4A and B). Duplication of the anterior spinal artery was identified. In addition, there was a suggestion of a small aneurysm near the nidus. 3D-RSA was performed at this time to confirm

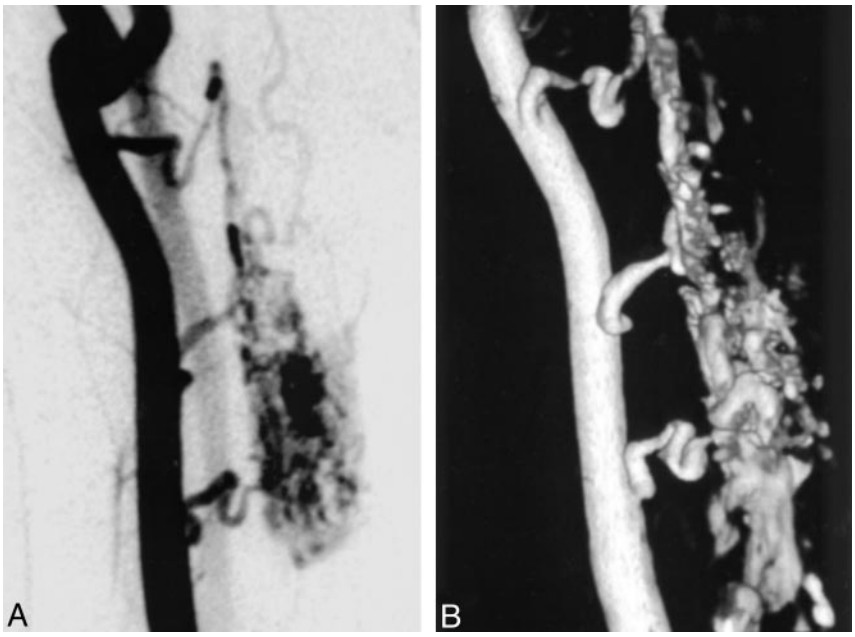

FIG 3. Patient 1, 20-year-old male patient with spinal cord AVM.

A, Lateral spinal angiogram of the left vertebral artery for this cervical AVM with contribution from multiple cervical levels.

B, 3D-RSA in the same projection as the prior study with enhanced detail in the course of the various feeding vessels. Note the depth of field created by the shadowing techniques provided in the software.

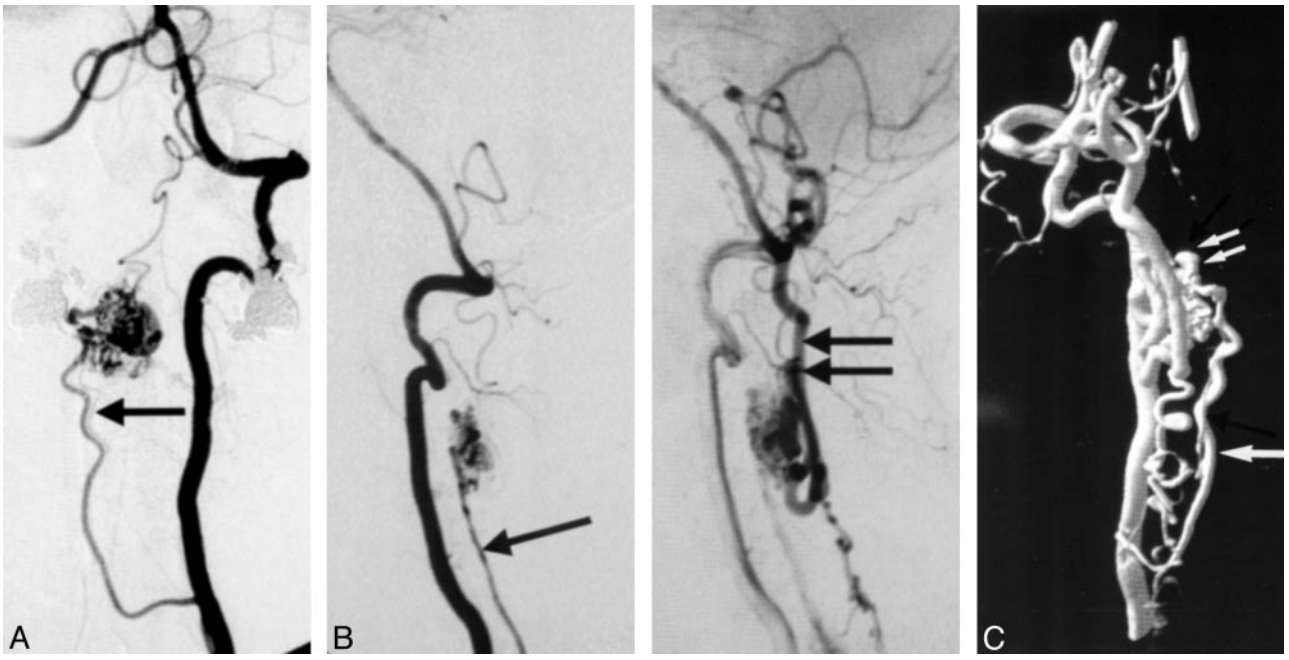

FIG 4. Patient 13, 51-year-old female patient with spinal cord AVM.

A, AP vertebral injection demonstrating supply to this cervical AVM from anterior and posterior spinal arteries. Note the duplication of the anterior spinal artery revealed by this view (*arrow*).

B, Lateral projection in the early (*left*) and late (*right*) arterial phases demonstrating the anterior spinal artery (*arrow* [early phase]) and the posterior draining vein (*double arrows* [late phase]).

C, 3D-RSA of the vertebral artery injection demonstrating resolution of fine details as depicted by the presence of the duplicated anterior spinal artery (*arrow*). Note the presence of the nidal aneurysm (*double arrow*).

the presence of this aneurysm (Fig 4C). 3D-RSA clearly demonstrates the presence of the aneurysm and its relationship to the malformation.

Discussion

Although first recognized as pathologic entities in 1888 (1), the modern era of diagnosis and treatment of spinal vascular malformations did not take place until the development of safe, selective spinal angiography (2). With the advent of this technique, a better preoperative understanding of the angioarchitecture of various vascular malformations of the spinal cord developed. Conventional angiography, however, is limited by its inability to clearly delineate the location of some of these pathologic vessels in relation to the spinal cord (eg, perimedullary versus intramedullary). While conventional MR imaging can be quite helpful

in determining the anatomic relationships of a malformation with the spinal cord and surrounding structures, it cannot clearly differentiate between artery and vein. Therefore, spinal angiography remains the reference standard. Its high-resolution dynamic imaging provides a vast amount of information that cannot be easily attained from less invasive techniques.

Although CT angiography and MR angiography provide excellent anatomic definition of intracranial vascular lesions comparable to that of DSA, these modalities have not been well developed for the evaluation of spinal vascular lesions. Indeed, the size of feeding vessels to these malformations is usually beyond the resolution of these modalities. The primary reason for this lies in the spatial resolution during image acquisition. In general, helical CT angiography acquires images with an average voxel size of $0.5 \times 0.5 \times 1.0$ mm. 3D-RSA, however, acquires images at a voxel size of approximately 0.2 mm at the isotropic center. These volumes can be processed in native or subtracted states. Furthermore, because of selective arterial injections during the time of acquisition, high contrast resolution (2000–7000 HU) is achieved. All of these factors contribute to the degree of spatial resolution that can be achieved with this technique.

As demonstrated in the case reports, 3D-RSA can provide information regarding location of the malformation relative to spinal cord. 3D-RSA was clearly helpful in determining the presence of aneurysms within the malformation that helped guide the goals of treatment (ie, treating the feeding pedicle that filled the venous aneurysm, as seen in case 4). In other instances, 3D-RSA helped the interventionalist better understand the complex and sometimes extremely tortuous vascular architecture of the malformation, so as to better direct the treatment plan. Furthermore, by modifying the relative transparency of the spine, a better understanding of the vessel's relationship to its surrounding structure is achieved. Stereoscopic views of the reconstructed images further our appreciation of these structures' complex relationships. Thus, in these 14 consecutive cases in which 3D-RSA was used, a variety of valuable information was gleaned from a single rotational view that would have otherwise required multiple oblique views.

In these 14 patients, we compared 3D-RSA with conventional DSA images, including several obique views. Although retrospectively identified on conventional angiograms, nidal and venous aneurysms were clearly better appreciated by means of 3D-RSA. On the basis of our experience in these cases, we are now comfortable performing oblique views only if indicated by 3D-RSA, which is performed after anteroposterior projections are obtained by conventional DSA. These indications include the suspicion of aneurysms and the attainment of a good working view for superselective catheterization and endovascular treatment.

The dose delivered to the patient during 3D-RSA has been studied. Whereas the dose delivered for the entire run is greater than a single-plane conventional run (3D-RSA, 316.8 μG/14 s; conventional single-plane angiography, 144 μG/20 s), the fact that oblique projections are not needed does reduce the overall dose to the patient (3D-RSA, 1.2 μG/frame; conventional single-plane angiography, 2.4 μG/frame). Furthermore, because of the capabilities inherent in the software which enable the interventionalists to variably opacify the surrounding bony structures, thin-section CT with reconstruction is not necessary, thus reducing the overall radiation and contrast medium load to the patient. In pretreatment situations, this study has occasionally been necessary in patients that cannot undergo MR imaging (claustrophobia or medical contraindications). Although conventional DSA does allow for variable opacification of the bony anatomy, ("landmark" function), it does not provide the 3D relationship of the vasculature to the bone. Postembolization rotational reconstruction is rarely used, (used once in this series); however, this technique can be beneficial. In the case of a spinal dural fistula (eg, patient 8), we occasionally perform postembolization CT to confirm venous penetration of NBCA mixture because venous penetration is sometimes difficult to evaluate by radiographic findings alone. Such a study helps us better predict the probability of recanalization of the fistula. 3D reconstruction of non-contrast rotational images of the NBCA cast can substitute for CT function, thereby reducing the patient's exposure to radiation.

Limitations of 3D-RSA exist. When imaging vascular lesions at the approximate level of the shoulders, the notable changes in penetration that occur when performing rotational angiography of the upper thoracic level limits the use of this technique. In addition, there are some logistical limitations in performing this technique in morbidly obese patients, which may minimally limit its utility. Although spatial resolution is less than 1 mm, it is still inadequate to discern some normal caliber spinal vasculature. Furthermore, as with conventional angiography, the use of 3D-RSA does not demonstrate *all* feeding vessels to an AVM with a single injection. Unlike conventional angiography, no temporal resolution exists when performing 3D-RSA; therefore, 3D-RSA cannot be used to determine whether there is increase in transit time within the anterior spinal artery. Although this lack of temporal resolution is one of drawbacks of the 3D-RSA, its use in conjunction with conventional DSA images helps to better distinguish between arterial and venous anatomy.

The use of 3D-RSA does not supplant conventional spinal angiography. Indeed, 3D-RSA is meant to enhance the interpretation of conventional spinal angiography by reducing (and at times eliminating) various oblique projections needed to interpret the anatomy in three dimensions.

Conclusion

3D-RSA is a safe and effective method of evaluating spinal vascular lesions and serves as an excellent adjunct to DSA. Image post-processing enables the

interventionalist to better determine the lesion's relationship with spinal cord and surrounding bony structures.

References

1. Gaupp J. **Hamorrhoiden der Pia mater spinalis im Geibiet des Lendenmarks**. *Beitr Pathol* 1888;2:516–518
2. Djindjian R. **Angiographie de la moelle epiniere.** *Acta Radiol (Diagn)* 1969;9:707–726
3. DiChiro G, Doppman JL, Ommaya A. **Selective arteriography of arteriovenous aneurysms of the spinal cord.** *Radiology* 1967;88: 1065–1077
4. Doppman JL. **Arteriography of the spinal cord.** *Semin Roentgenol* 1972;7:231–239
5. Turjman F, Bendib K, Girerd C, et al. **Pretherapeutic evaluation of intracranial aneurysms using three-dimensional angiography (3D morphometer): preliminary results.** In: Taki W, Picard L, Kikuchi H, eds. *Advances in Interventional Neuroradiology and Intravascular Neurosurgery.* Amsterdam: Elsevier Science;1996;75–79
6. Anxionnat R, Bracard S, Macho J, et al. **3D angiography: clinical interest and first applications in interventional neuroradiology.** *J Neuroradiol* 1998;25:251–262